A Case Study of Three Different Brake Pads Used in Iranian Rail Systems

A. Nasr[1], M. H. Esnaashary[1,2]

[1] *Train Brake Reference Laboratory (TBRL), School of Railway Engineering, Iran University of Science and Technology, Tehran, Iran.*
[2] *School of Metallurgical and Materials Engineering, Iran University of Science and Technology, Tehran, Iran.*
Received: 02 January 2019 - Accepted: 15 March 2019

Abstract

Brake system and its components are of high importance in rail transportation systems. In this regard, brake linings, pads and blocks are especially important and this is why periodic evaluation of these parts is common practice in all rail systems. In this paper, some characteristics of three types of brake pads (friction materials in disc type brake mechanism) named types A, B and C (not to reveal the brand types) used in Iranian railways are compared against each other. Type A is an European product and the other two are Iranian pads manufactured domestically at different stages (type B is a new product and type C is an old one). The surface of pads, its compound, density, porosity, water adsorption, and impact strength and friction coefficient are evaluated. By comparing the results, it is appeared that the European brake pad possessed the lowest porosity, the highest impact strength and variation of its friction coefficient was more stable than the others. In addition, the performance of the type C compared with type B seemed to be much better in regard to wear rate and impact strength.

Keywords: Rail Brake, Friction Lining, Rail Safety, Brake Pads, Iranian Railways Industries, Wear.

1. Introduction

Train brakes include different types such as air (pneumatic) brake, dynamic brake, magnetic brake and eddy current brake. However, the air brake system is more commonly used as main brake systems in all rail vehicles. In trains equipped with the air brake (its schematic is shown in (Fig. 1.), every vehicle is provided with a car distributor valve [1]. This device modulates the pressure inside brake cylinder according to a law that is proportional to the difference between the pressure in the air brake pipe and the reference pressure stored in the command reservoir unit. Braking signal in the brake pipe is generated by the driver using a brake valve. In air brake system, braking of the train starts by reducing the air pressure (introducing brake signal) in the train main air brake pipe [2]. This is applied by the brake control valve located in the locomotive cab. By reducing the air pressure in the main pipe, the distributor valve of each car becomes excited which causes flow of the air from the car auxiliary air reservoir to the brake cylinder. The produced cylinder trust then is transmitted, by use of a rigging system, to vehicle's braking mechanism [3].
In rail brake system, there are usually two different disc braking and tread braking mechanisms (Fig. 2.) with their advantages and disadvantages. The tread braking action is carried out by pressing friction materials, in this case referred as blocks, against the tread of the rotating wheels.

*Corresponding author
Email address: mh.esnaashary@yahoo.com

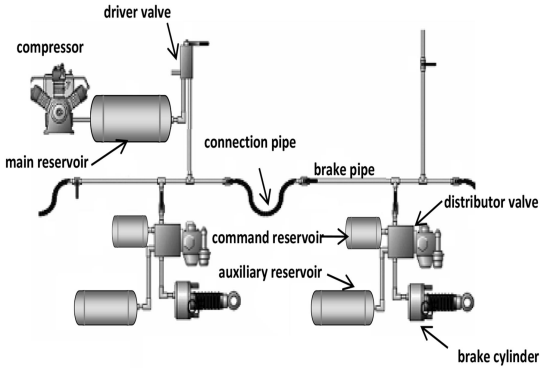

Fig. 1. Schematic of automatic air brake system [1] .

Friction force induced in braking mechanism then causes braking effort to speed down the rotating wheels of the vehicle. In disc type mechanism, the braking force is introduced by pressing friction materials, in this case referred as pads, against rotating discs which are fixed on the axles [1,2].

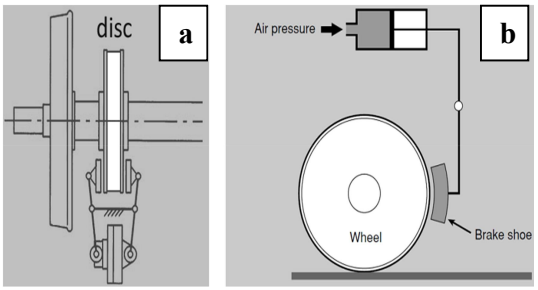

Fig. 2. Schematic of a) disc and b) tread braking mechanisms [4].

Friction materials (linings) used in brake systems can be divided into three major types including metallic, carbon-based and organic types. Organic types is itself subdivided into asbestos, non-asbestos and semi-metallic linings (SML[1]) [5]. The non-asbestos linings are mainly used on conventional road cars though the other linings are used in much heavier applications. For instance carbon-based types are basically used in racing cars and airplanes [5,6] , the metallic one for high-speed trains [7] and the SML for conventional passenger trains.

Friction materials need to possess suitable coefficient of friction (COF) with low variation at different thermal conditions. Acceptable COF of pads places between 0.3 and 0.6. At very high COF the wear of the discs increases fast and at low values of COF the safety of the braking reduces. Moreover, the wear of the paring materials (discs and pads) should be in desired standard figures. It is of high importance that the friction materials of the pads should not contain any species threatening human and environmental health [8].

A literature review suggests that the SML are mainly composed of four main parts namely: binder (fixing part), fibres (reinforcing part), friction additives and fillers (four F formula) [9]. Researchers in last two to three decades have been trying to manipulate different components and their magnitude to reach required characteristics of the SML [8]. The focus of scientists and researchers in rail brake friction material is due to the deep development in train transportation in regard to speed, axle load, shorter head ways and also environmental issues. Hong et al. [10] modified phenolic resin by Si and B-P and attained increased COF and enhanced its fade resistance. Wang et al. evaluated addition of latex to phenolic resin by the laboratory [11,12] and practical assessments [13] and found that the use of latex improved integrity and impact strength of the friction materials. Liu et al. [14] added different type of rubbers including SBR, VPR, NBR and CNBR to the resin. The results showed that the decomposition temperature of the friction materials decreased slightly though its impact strength improved significantly. Jang et al. [15] stabilized COF of SML through replacing iron fibres by copper fibres. Kim et al. [16] indicated complementary role of graphite and antimony tri-sulfide as friction additives and expressed that simultaneous presence of the additives in pads improved COF stability at different thermal conditions. In another research [17], the triple roles of hard particles of SiC on friction behaviour of pads was evaluated. The coarse SiC particles played the role of reinforcement agent, grinding to micro-scale during wear process resulting abrasive wear and thirdly by more grinding the nanoparticles were produced and entered friction film resulting improved strength and stability of the film against wear.

The most considered environmental issues in braking attributes to squealing and airborne particles. Squealing is an annoying and discomforted sound created from friction of pad and disc that can induce dissatisfaction to the passengers during using transportation systems. It comes from two sources: 1) dynamic instability in brake system and 2) pad and disc composition [18]. For example, Kchaou et al. [19] indicated how the presence and non-presence of brass filler can affect squealing and Wang et al. [20] showed the effect of surface roughness on it. On the other hand, friction of pad and disc and entrapped external dust particle between them can create airborne particles that affect passenger health. According to the reports [21,22], the main part of the particle composed of Fe and C.

Due to the importance of the friction material on safety of rail services, periodic assessment of the brake pads is essential. In this study, the authors decided to evaluate three types of rail pads used in Iranian rail transportation; an European pad and two local manufactured ones.

2. Materials and Methods

Three types of rail brake pads used in Iranian railway industries were selected and named as A, B and C. Type A is an European brand and B and C refer to locally manufactured types, newly and previously manufactured respectively. Their compositions were assessed using X-ray diffractometer XRD (DRON-8, Bourevestnik, Russia). In addition, a piece of each pad was heated to 450°C for 2 h and for decomposing its binder. Then the disintegrated compounds were tested using scanning electron microscopy SEM (VEGA II, TESCAN, Czech).

Density of pads was measured applying Eq. (1). [23]:

$$\rho = \alpha / (\alpha + w - b) \quad \text{Eq. (1)}$$

where ρ is specific density (g/cm3), α is sample weight in air, w is wire weight and b is weight of sample and wire in water (all of them in g). The amount of apparent porosity was then determined by Eq. (2). [24]:

$$\text{apparent density} = (m_3 - m_1) \times 100 / (m_3 - m_2) \quad \text{Eq. (2)}$$

where m_1 is sample weight in dry condition, m_2 is immersed sample weight and m_3 is sample weight in wet condition (all of them in g).

According to ASTM D570 standard, the amount of adsorbed water and weight loss in water was measured. Three types of weight were measured, including dry sample weight after heating at 110°C

[1] Semi-Metallic Lining

for 1 h, wet sample weight after immersing it for 24 h in water and dry sample weight after heating at 110°C for 1 h. They referred to d, f, and e respectively. Water adsorption and sample weight loss in water is then determined by the following Eq. (3). and Eq. (4). [25]:

$$\text{Water Adsorption} = f - d / d \quad \text{Eq. (3)}$$

$$\text{Sample Weight Loss in Water} = d - e / d \quad \text{Eq. (4)}$$

Impact strength of pads was determined according to ASTM E23 standard for non-notched sample and with the dimension of 4×10×80 mm [26].

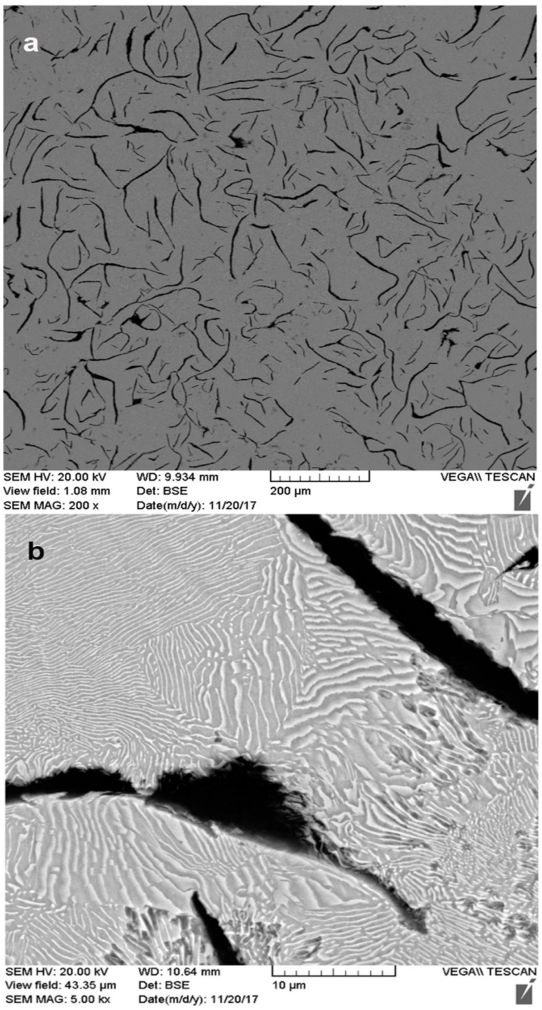

Fig. 3. Micrographs of grey cast iron disc that indicate the network of worm-like graphite (a) and pearlite lamellar structure (b).

Grey cast iron was used as disc to evaluate wear of the pads against it. Micrographs taken of the used grey cast iron disc are shown in Fig. 3. In this figure, the black worm-like structure indicates graphite and the layers of the finger-print structure between graphite flakes show pearlite structure of the matrix. The pearlite grey cast iron is usually selected as disc composition in rail brake systems because of its preferable thermal conduction due to the connected structure of the worm-like graphite and because of the application of its graphite as a lubricant during wear process [27].

The amount of wear rate and COF were measured based on ASTM G99 standard by the wear of a pin with 10 mm diameter on the grey cast iron disc with 50 mm diameter (the used instrument is shown in Fig. 4.). The applied forces of 200 and 300 N at speed of 0.12 m/s during 450 m were selected. The worn surface was observed by SEM and wear rate was determined by Eq. (5). [28]:

$$S_w = \Delta m / (F_f h) \quad \text{Eq. (5)}$$

where S_w is wear rate in g/Nm, Δm is weight variation in g, F_f is friction force in N and h is distance in m [29].

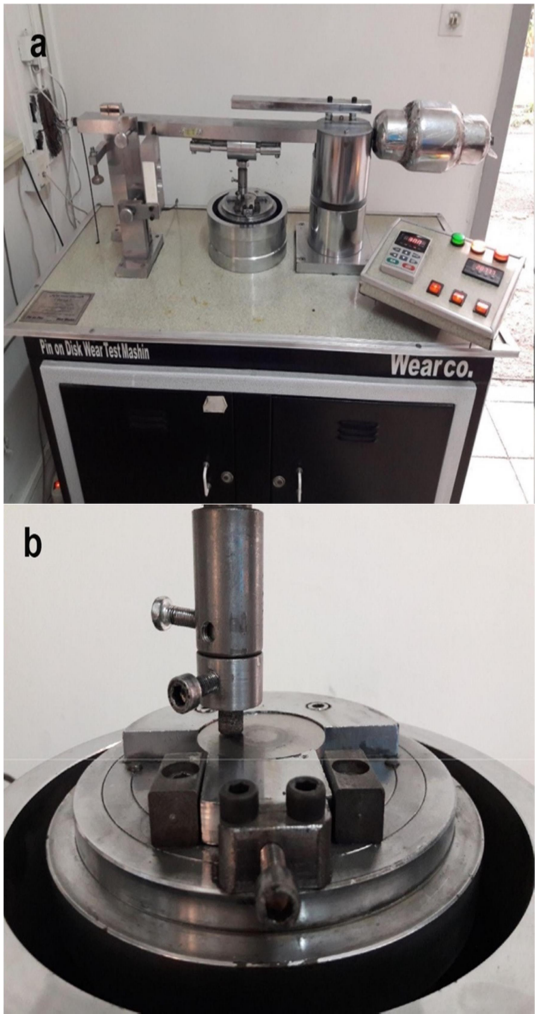

Fig. 4. The view of wear test instrument (a) and placement of the pin created from the pads against grey cast iron disc (b).

3. Results and Discussion

3.1. Characteristic Evaluation

Fig. 5. Shows XRD patterns of the pads A, B and C and Fig. 6., Fig. 7. and Fig. 8. presents their constructed compounds.

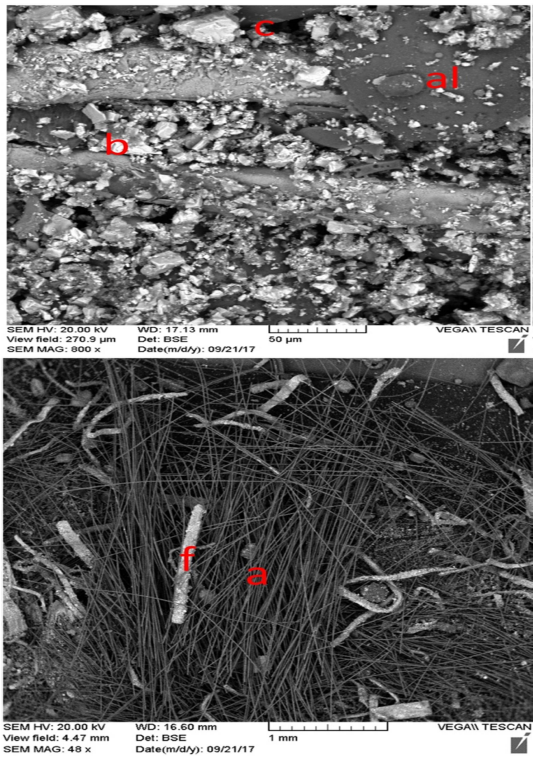

Fig. 6. Micrographs of the component of sample A (European pad). a, f, al, c and b referred to Ca-Al-Si-O, Fe_2O_3, Al_2SiO_5, C and $BaSiO_4$, respectively, based on XRD and EDS results.

As can be seen, fibre glass Ca-Al-Si-O as a reinforcement agent with the dimension of 3-4 mm in length and 11 µm in diameter are used in pad A. In addition, iron oxide fibres Fe_2O_3 with the dimension of 1-2 mm in length and 150 µm in diameter are also used as reinforcing material. Barium sulfate particles $BaSO_4$ of the size 15 µm and graphite particles as lubricants, silicon di-oxide SiO_2, magnesium oxide MgO, iron particles and aluminum silicate Al_2SiO_5 as abrasives are used.

In samples B and C iron fibres with dimension of 2-4 mm in length and 150-200 µm in diameter. As lubrication, 20-100 µm graphite and barium sulfate together with SiO_2, MgO and also Al_2SiO_5 as abrasive agents can be observed.

The amount of density, water adsorption, weight loss in water and impact strength measured for the pads presented in Table. 1. The density of sample A is about 2.2 g/cm^3 and for both samples B and C are measured to be approximately 1.9 g/cm^3.

Table. 1. Density, apparent porosity, water adsorption, weight loss in water and impact strength of the samples A (European pad), B (new local pad) and C (old local pad).

Sample	Density (g/cm^3)	Apparent Porosity (%)	Water Adsorption (%)	Weight Loss in Water (%)	Impact Strength (kj/m^2)
A	2.26 ± 0.01	10.7 ± 0.3	5.43 ± 0.08	0.10 ± 0.06	12.50 ± 1.44
B	1.90 ± 0.05	13.8 ± 2.1	9.05 ± 1.71	-0.37 ± 0.07	5.83 ± 0.83
D	1.86 ± 0.06	15.1 ± 2.4	10.27 ± 1.79	-0.10 ± 0.10	10.00 ± 0.00

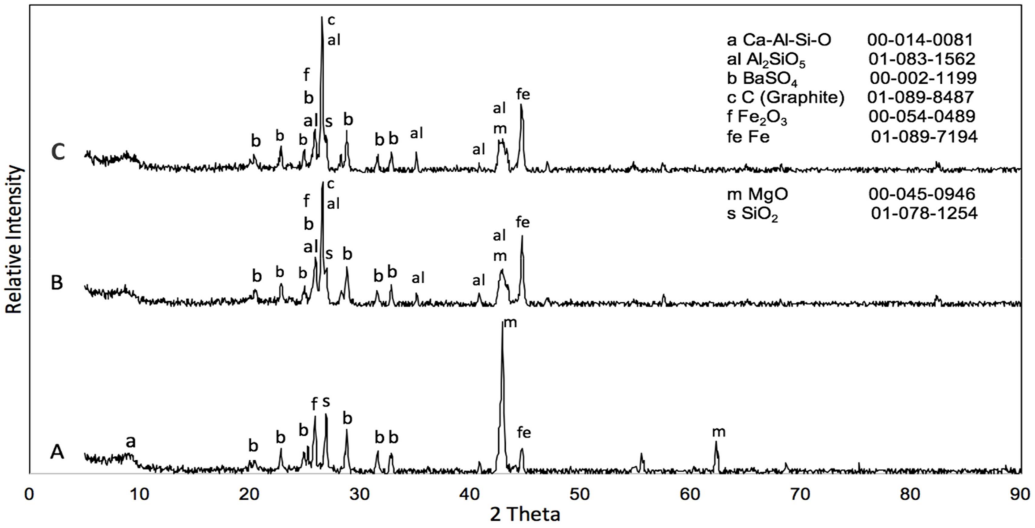

Fig. 5. XRD patterns of sample A. (European pad), B. (new local pad) and C. (old local pad).

The lower density of these pads could be related to the higher amount of graphite and their porosity. Water adsorption in sample B and C are about twice that of sample A. The difference can be resulted from water adsorption of graphite, trapping water in the surface porosity and hydration of iron fibres. The amount of weight loss in water was ignorable in all the samples.

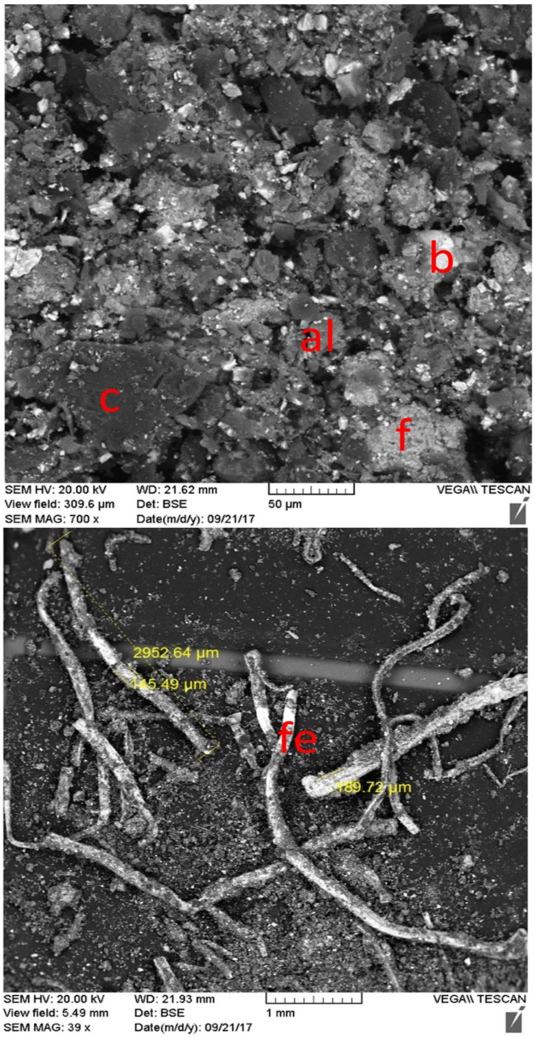

Fig. 7. Micrographs of the component of sample B (new local pad). f, fe, al, c and b referred to Fe_2O_3, Fe, Al_2SiO_5, C and $BaSiO_4$, respectively, based on XRD and EDS results.

This indicates that the crosslinking process during the curing process was approximately completed and the soluble monomers are not present in the water. In regard to impact strength, it is seen that the value of this property for sample A is significantly higher than that of the others. The minimum measured value of the impact strength is above the standard figures in rail industry. Impact strength can

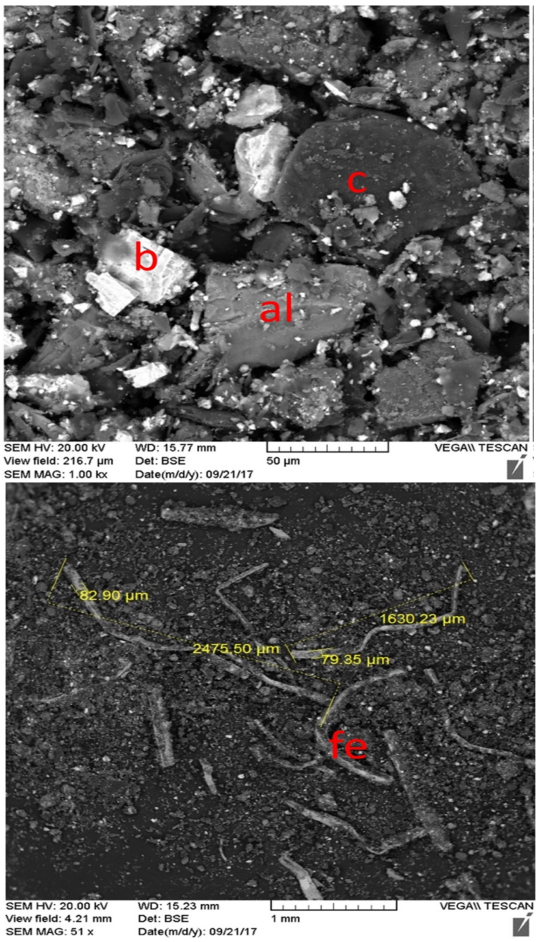

Fig. 8. Micrographs of the component of sample C (old local pad). fe, al, c and b referred to Fe, Al_2SiO_5, C and $BaSiO_4$, respectively, based on XRD and EDS results.

be considered as the strength of the binder to preserve the integrity of pad structure. The all samples show acceptable impact strength but their differences could be originated from two sources. In sample A, the low-diameter glass fibres have filled the space among the thick iron oxide fibres improving the impact strength. In sample B and D however the presence of higher amount of porosity originated from manufacturing process might be a reason for lower impact strength.

The measured friction coefficients measured for three pads using pin-on disc devices are shown in Fig. 9 and Fig. 10. at 200 and 300 N force respectively. It seems that at 200 N, the sample A with average COF of about 0.26 possessed more stable COF. The average COF for sample B and C, about 0.27 and 0.26 respectively, was not significantly different from that of sample A though their show less stability. The running-in length for sample A, B and C are about 10, 25 and 3 m respectively. At compression force of 300 N, COF variation is divided into two sections.

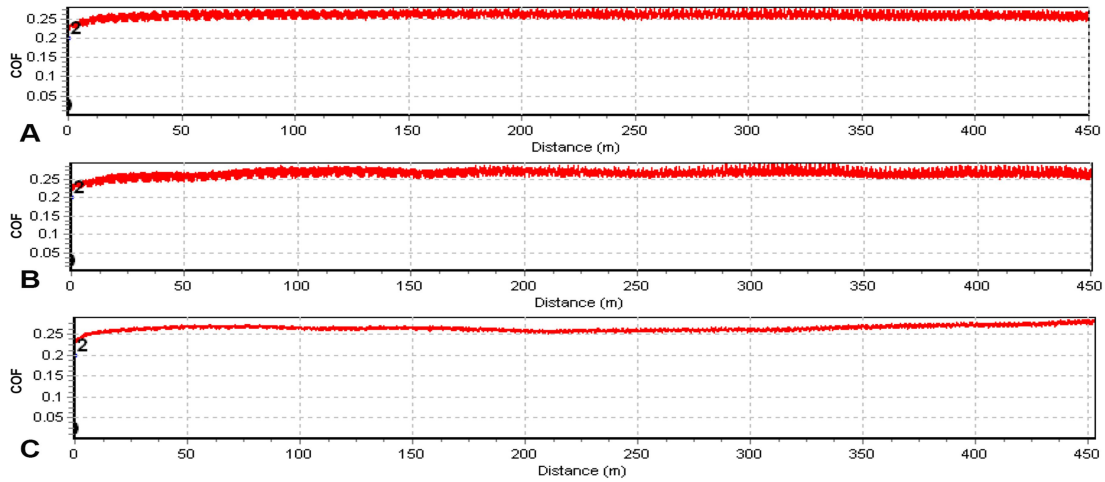

Fig. 9. Results of wear test (coefficient of friction-distance) of sample A. (European pad), B. (new local pad) and C. (old local pad) on grey cast iron disc performed at the force of 200 N and the speed of 0.12 m/s.

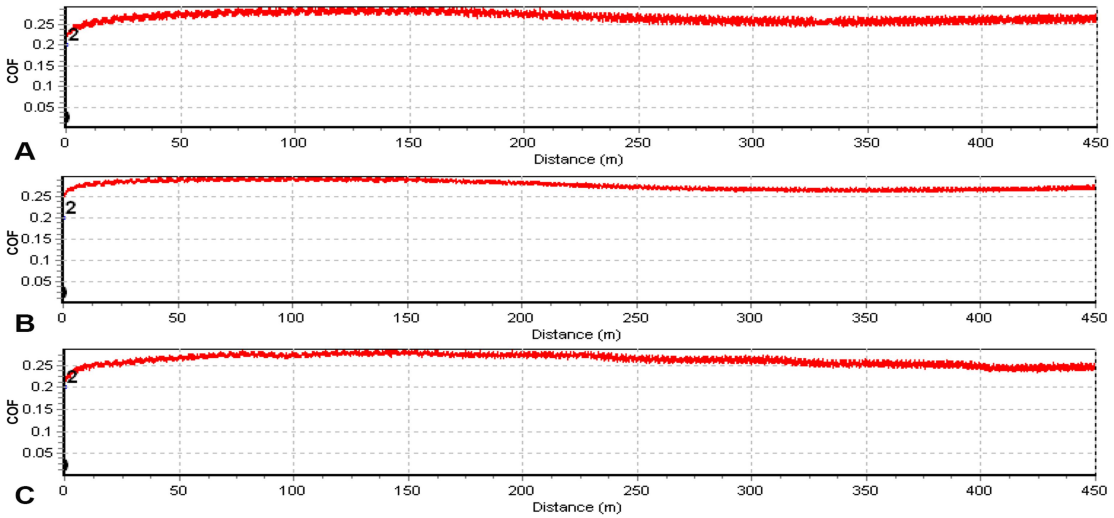

Fig. 10. Results of wear test (coefficient of friction-distance) of sample A. (European pad), B. (new local pad) and C. (old local pad) on grey cast iron disc performed at the force of 300 N and the speed of 0.12 m/s.

At the first section, COF of about 0.27, 0.29 and 0.27 for A, B and C pads respectively is higher than those of the second section. In the later section COF is about 0.26, 0.27 and 0.25 for sample A, B and C respectively. The observed differences are judged by evaluating wear surface under SEM in the coming discussions.

3.2. Microstructural Evaluation

Surface micrographs for the all three worn pads are shown in Fig. 11. and Fig. 12. at 200 and 300 N respectively. At 200 N forces, it is observed that the low-friction resistance additives worn out of the matrix are accumulated beside the reinforcement fibres in all pads. However, at 300 N of Fig. 12., the accumulated particles stuck to each other and improved the contact surface of the pad and disc for pad A. The increased contact surface causes lower pressure and hence decreases the amount of wear. In addition, the integration of particles in a friction film with lower shear strength and lower individual presence of worn particles declines COF. In sample B and C, the disintegrated particles are also accumulated beside reinforcement fibres however high number of cracks is observed in the friction film. The observed cracks in the friction films is an indication of low integrity of the worn material in the films which itself causes lower strength there. This phenomenon disintegrates the film under pressure producing some particles that cause high

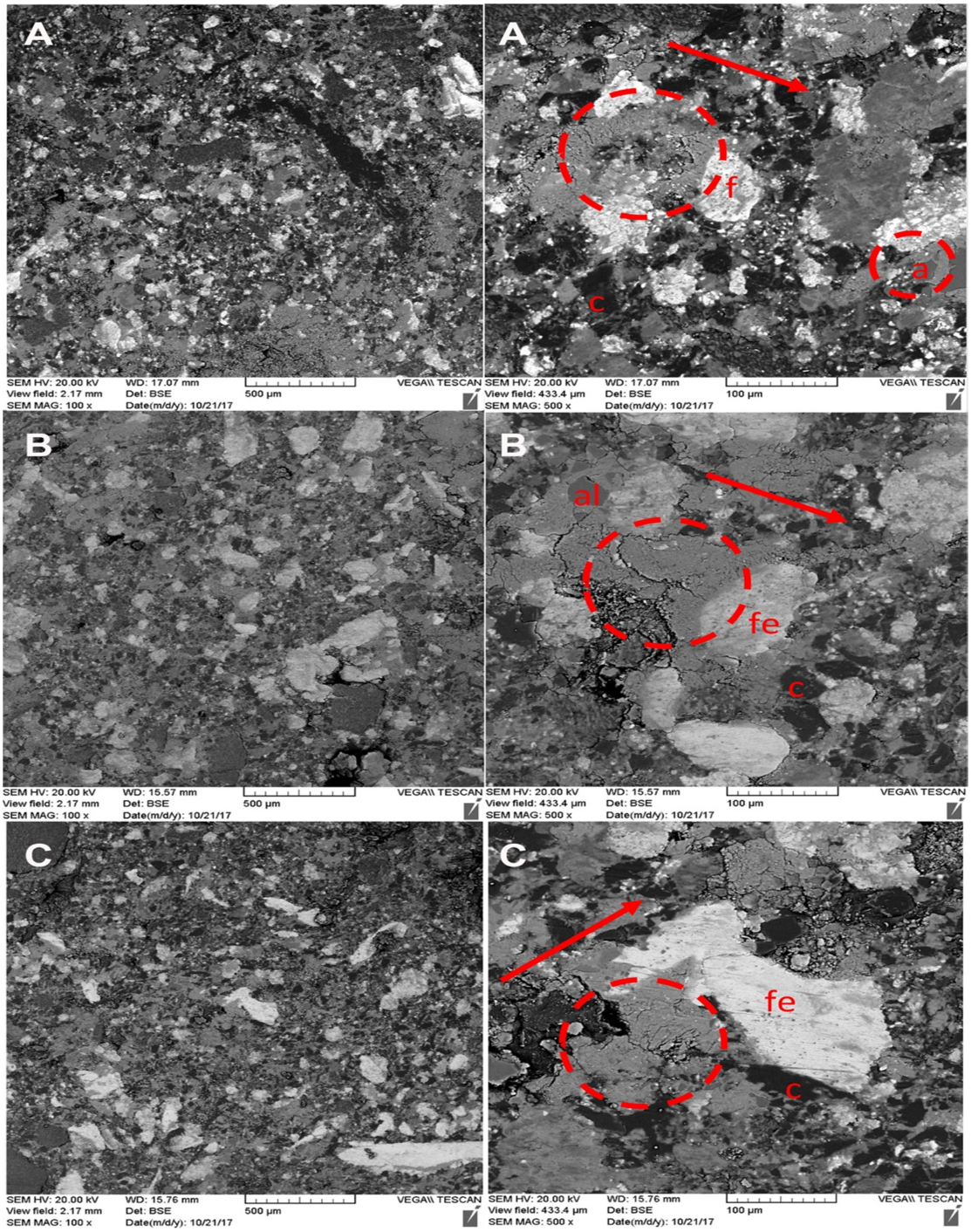

Fig. 11. Micrographs of samples A. (European pad), B. (new local pad) and C. (old local pad) after wear test under force of 200 N and speed of 0.12 m/s. The red dashed circles indicate the position of particle accumulation beside reinforcement fibres and the red arrow show the direction of wear test.

variation in COF and noisy braking. Fig. 11. and Fig. 12., show that in all the sample there exists no significant differences in the number of iron reinforcement fibres. This indicates that the differences in the friction films might not be related to iron fibres. As mentioned above, the presence of thin glass fibres in sample A around the thick iron fibres enhances integrity and strength of this sample. It then might be judged that the presence of the cracked friction films in samples B and C could be resulted from the lack of the glass fibres in their composition.

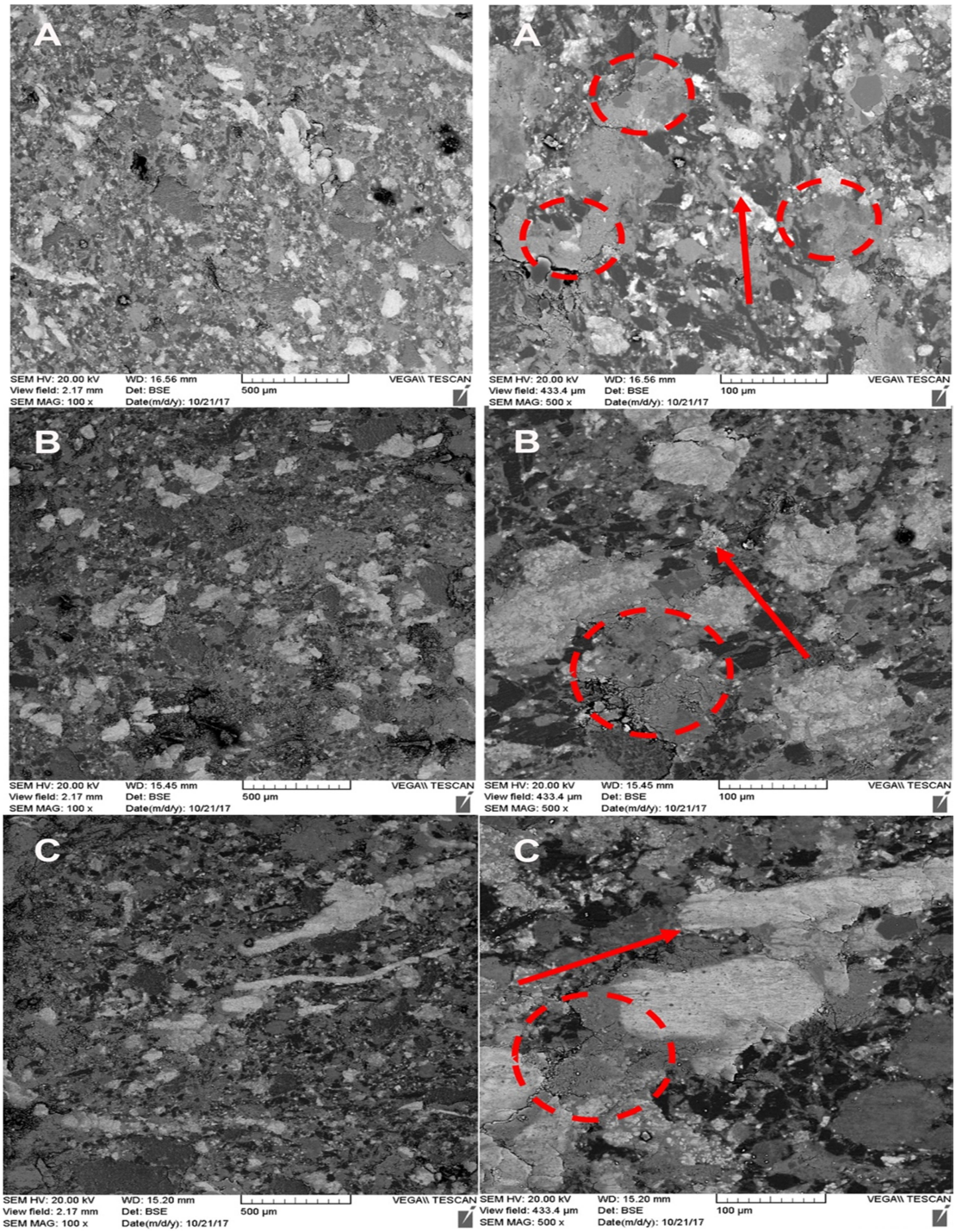

Fig. 12. Micrographs of samples A. (European pad), B. (new local pad) and C. (old local pad) after wear test under force of 300 N and speed of 0.12 m/s. The red dashed circles indicate the position of particle accumulation beside reinforcement fibres and the red arrow show the direction of wear test.

In the lack of the glass fibres, the worn-out particles accumulate only close to the iron fibres. Then applied pressure on the pads exerts on a limited contact surface resulting crack of the friction film. It should be mentioned that the presence of other additives of the pads not detected by the performed analysis can affect the behaviour of the friction films.

The wear rates of the samples are reported for 200 and 300 N force in Table. 2. As can be seen the wear rate of the sample B is considerably higher than those of samples A and C for different applied force.

It is also seen that the wear rate at 200 N forces is slightly higher for sample C than for sample A though the rate is the same at 300 N for these two samples. These observations are due to the differences mentioned above regarding the samples.

Table 2. Wear rate of the samples A. (European pad), B. (new local pad) and C. (old local pad) at 200 and 300 N forces.

Force (N)	200	300
Pad A	1.600	2.000
Pad B	2.600	2.700
Pad C	1.900	2.000

From the observed phenomena and discussions made above, it seems that the sample A performs better than the other two samples in regard to wear rate, impact strength, and porosity and water adsorption. Furthermore, the usage of iron fibres in the sample B and C compared the usage of iron oxide fibres in the sample A can create some problems by wear against cast iron disc. As mentioned by Jang et al. [15] the composition resemblance between friction paring (here cast iron disc and iron fibre of samples B and C) could cause material infusion which is a major defect in air brake systems as the cause some damages to the discs. The results showed that the better quality of samples C compared to sample B, having similar compositions, indicated that the production process and end of line production quality control could be a major issue to be considered. However, a more laboratory analysis and filed investigations are needed to judge about their overall performance and quality.

4. Conclusions

Brake linings (pads and blocks) are very important in the safety and environmental issues of all rail systems. There have been important research endeavour in investigating brake lining in recent years. It is believed that there are huge expenses due to low quality of friction materials in some rail systems. In this paper, some characteristics of three types of brake pads named types A, B and C used in Iranian railways were compared against each other. Type A is an European product and the other two are Iranian pads that B and C are the new and old product of the same factory. The highlighted results of this study are as follows:

1. This study showed that sample A performs better than samples B and C in regard to wear rate, impact strength, porosity and water adsorption.
2. The usage of iron fibres in the sample B and C compared the usage of iron oxide fibres in the sample A can create some problems by wear against cast iron disc.
3. The results also indicate that the better quality of samples C compared to sample B showed that the production process and quality control during manufacturing could be a major issue to be considered.
4. It should be mentioned that a more laboratory analysis and filed investigations are needed to judge about the overall performance and quality of the three samples investigated in this paper.

References

[1] S. Mohammadi and A. Nasr, Int. J. Veh. Syst. Model. Test., 5(2010) 176.
[2] A. Nasr and S. Mohammadi, Proc. Inst. Mech. Eng. Part F J. Rail Rapid Transit, 224(2010) 523.
[3] S. Mohammadi and R. Serajian, Mech. Ind., 16(2015) 205.
[4] I. Hasegawa and S. Uchida, Japan Railw. Transp. Rev., 20(1999) 52.
[5] A. E. Anderson, Friction and Wear of Automotive Brakes, in ASM Handbook Volume 18, Friction, Lubrication, and Wear Technology, ASM International, (1992) 569.
[6] E. M. Tatarzycki and R. T. Webb, Friction and Wear of Aircraft Brakes, in ASM Handbook Volume 18, Friction, Lubrication, and Wear Technology, ASM International, (1992) 582.
[7] P. Dufrénoy and D. Weichert, J. Therm. Stress., 26(2003) 815.
[8] X. Xiao, Y. Yin, J. Bao, L. Lu, and X. Feng, Adv. Mech. Eng., 8(2016) 1.
[9] M. Eriksson, F. Bergman, and S. Jacobson, Wear, 252(2002) 26.
[10] U. S. Hong, S. L. Jung, K. H. Cho, M. H. Cho, S. J. Kim, and H. Jang, Wear, 266(2009) 739.
[11] H. Wang, X. Wu, X. Liu, and P. Cong, J. Macromol. Sci. Part A, 48(2011) 261.
[12] H.-Q. Wang, X.-Y. Wu, T.-S. Li, X.-J. Liu, and P.-H. Cong, J. Appl. Polym. Sci., 126(2012) 1746.
[13] H. Wang, G. Zhuang, C. Wang, and S. Zheng, J. Macromol. Sci. Part A, 48(2011) 531.
[14] X. Liu, H. Wang, X. Wu, J. Bu, and P. Cong, J. Macromol. Sci. Part B-Physics, 53(2014) 707.
[15] H. Jang, K. Ko, S. Kim, R. Basch, and J. Fash, Wear, 256(2004) 406.
[16] S. J. Kim, M. Hyung Cho, K. Hyung Cho, and H. Jang, Tribol. Int., 40(2007) 15.
[17] V. Matějka, Y. Lu, Y. Fan, G. Kratošová, and J. Lešková, Wear, 265(2008) 1121.
[18] A. R. M. Lazim, M. Kchaou, M. K. A. Hamid, and A. R. A. Bakar, Wear, 358–359(2016) 123.
[19] M. Kchaou, A. Sellami, A. R. Abu Bakar, A. R. M. Lazim, R. Elleuch, and S. Kumar, Steel Compos. Struct., 19(2015) 939.
[20] D. W. Wang, J. L. Mo, H. Ouyang, G. X. Chen, M. H. Zhu, and Z. R. Zhou, Mech. Syst. Signal Process., 46(2014) 191.
[21] T. Moreno, X. Querol, V. Martins, M. C. Minguillón, C. Reche, L. H. Ku, H. R. Eun, K. H.

Ahn, M. Capdevila, and E. de Miguel, Environ. Sci. Process. Impacts, 19(2017) 59.
[22] V. Martins, T. Moreno, M. C. Minguilln, B. L. Van Drooge, C. Reche, F. Amato, E. De Miguel, M. Capdevila, S. Centelles, and X. Querol, Environ. Pollut., 208(2016) 125.
[23] ASTM Standard D792, Standard Test Methods for Density and Specific Gravity (Relative Density) of Plastics by Displacement, (2013).
[24] ISO Standard 5017, Dense shaped refractory products Determination of bulk density, apparent porosity and true porosity, (2013).
[25] ASTM Standard D570, Standard Test Method for Water Absorption of Plastics, (2018).
[26] ASTM Standard E23, Standard Test Methods for Notched Bar Impact Testing of Metallic Materials, (2018).
[27] G. Cueva, A. Sinatora, W. L. Guesser, and A. P. Tschiptschin, Wear, 255(2003) 1256.
[28] ASTM Standard G99, Standard Test Method for Wear Testing with a Pin-on-Disk Apparatus, (2017).
[29] P. D. Neis, N. F. Ferreira, and J. C. Poletto, J. Brazilian Soc. Mech. Sci. Eng., 38(2016) 1935.